Distribution Agreement

In presenting this thesis or dissertation as a partial fulfillment of the requirements for an advanced degree from Emory University, I hereby grant to Emory University and its agents the non-exclusive license to archive, make accessible, and display my thesis or dissertation in whole or in part in all forms of media, now or hereafter known, including display on the world wide web. I understand that I may select some access restrictions as part of the online submission of this thesis or dissertation. I retain all ownership rights to the copyright of the thesis or dissertation. I also retain the right to use in future works (such as articles or books) all or part of this thesis or dissertation.

Signature:

_____	_____
Siying Cen	Date

BACTERIAL LIPIDS INDUCED AMYLOID ASSEMBLY AND DISEASE ETIOLOGY

By

Siying Cen

Master of Science

Chemistry

_____

Dr. David G. Lynn
Advisor

_____

Dr. Vincent P. Conticello
Committee Member

_____

Dr. James Kindt
Committee Member

Accepted:

_____

Lisa A. Tedesco, Ph.D.
Dean of the James T. Laney School of Graduate Studies

_____ Date

BACTERIAL LIPIDS INDUCED AMYLOID ASSEMBLY AND DISEASE ETIOLOGY

By

Siying Cen

B.S., Wuhan University, 2016

Advisor: David G. Lynn, PhD.

An abstract of

A thesis submitted to the Faculty of the

James T. Laney School of Graduate Studies of Emory University

in partial fulfillment of the requirements for the degree of

Master of Science

in Chemistry

2018

Abstract

Amyloid has been connected with protein misfolding diseases from the beginning, yet no clear mechanism for neurodegenerative diseases is currently proposed. One proposal is that the gut microbiome plays a role in the formation of amyloid plaques in the human brain. To evaluate the hypothesis that lipopolysaccharides (LPS) from gram-negative bacteria's membrane participates in the Alzheimer's disease (AD) at the molecular level, I have tested a model for β-amyloid (Aβ) peptides associating with LPS from gram-negative bacteria membrane, specifically determining whether the lipid A from LPS co-assembles with Aβ (16-22), the nucleating core of Aβ, and its congeners. In the experiments, lipid A and Aβ (16-22) were co-assembled in both aqueous and organic solutions, and the resulting structures characterized with TEM and ATR-FTIR. A type of glycerophospholipid, phosphatidylinositol (PI), was employed as a more soluble and simplified lipid A to mimic the co-assembling of lipid A and Aβ (16-22). My experiments demonstrate a direct interaction between LPS and Aβ (16-22) and CD results support the ability of LPS to induce β-sheet formation in soluble amyloid peptides. In summary, my research supports a direct association between Aβ peptides and LPS, the main component of bacterial outer membrane, but further experiments are needed to reveal the mechanism of LPS-Aβ peptides interaction, which may help explain the etiology of Alzheimer's disease and bacterial toxicity.

Bacterial Lipids Induced-Amyloid Assembly and Disease Etiology

By

Siying Cen

B.S., Wuhan University, 2016

Advisor: David G. Lynn, PhD.

A thesis submitted to the Faculty of the

James T. Laney School of Graduate Studies of Emory University

in partial fulfillment of the requirements for the degree of

Master of Science

in Chemistry

2018

ACKNOWLEDGMENTS

First of all, I would like to express my deep gratitude towards my advisor, Professor David G. Lynn. During my graduate studies, he has been a mentor for both science and life. He fueled my curiosity, encouraged me to ask bold questions, and led me to explore mystery of science. His enthusiasm towards education and academy helped me to become a independent researcher. I'm also thankful for my second committee advisors, Professor James Kindt and Professor Vincent P. Conticello for being my role model in science and providing insightful suggestions to my research projects.

For conducting experiments, I would first like to thank Dr. Chen Liang, Dr. Ming-Chien Hsieh and Dr. Meth Anil for not only teaching me critical experiments patiently, but also having the wisdom to provide valuable suggestions and break many bottle necks. They are all good mentors and models to my research and life. Additionally, I'm grateful for Dr. Hong Yi, Dr. John Bacsa and Dr. Shaoxiong Wu for their generous guidance with TEM, X-ray diffraction and NMR experiments.

I've enjoyed such a great time to work with so many colleagues at Lynn lab. Dr. Chen Liang and Dr. Ming-Chien Hsieh are my elder friends. Dr. Meth Anil, Dr. Olga Taran, Dr Yushi Bai, Dr. Noel Li, Dr. Rolando Rengifo and Anthony Sementilli are my mentors and offered great guidances. Many thanks to Youngson Kim, Mandy Chen and Christella Gordon for your company. Your presence makes Lynn's lab into my second family.

Beside research, I am lucky to make friends with many graduates at Emory and brothers and sisters in church. I am not able to list their names here one by one, but I am thankful for their support and company in my graduate studies and life. My friends not only help me overcome countless obstacles, but also share my happiness as well as sorrow.

Finally, I would like to address my thanks to my Father Hua Cen and my Mother Yuhua Lyu for supporting my dream and loving me unconditionally. You are my belief to face the world bravely.

Table of Contents

List of Figures

List of Tables

Chapter 1. Background

Bacteria and neurodegenerative diseases

Amyloid protein misfolding and aggregation has been shown to be associated with a number of incurable neurodegenerative diseases such as Alzheimer's disease (AD), Parkinson's disease, and Creutzfeldt-Jacob syndrome [1]. The major amyloid peptide involved in each prion disease is different; for AD, it is β-amyloid (Aβ) peptides Aβ(1-40/42) [2]. The mechanism of protein misfolding is unclear, but some recent studies have revealed that there may be a link between bacteria and amyloid disorders. For example, gut bacteria can regulate motor dysfunction as exemplified by Parkinson's disease (PD) in mice [3], and bacteria can be detected in human brains [4]. A recent report even demonstrated that lipopolysaccharides (LPS) and pili proteins from *E coli* colocalize with Aβ amyloid plaque in human AD brains [5]. Based on these findings, defining the interaction of Aβ peptides with LPS could reveal a molecular correlation between Alzheimer's disease and bacteria.

Alzheimer's disease and the amyloid peptide self-assembly

The hallmark of Alzhermer's desease is the presence of amyloid plaques accompanied with damaged neurons in the brains [34]. Among all the materials found in amyloid plaques, β-amyloid peptides, $A\beta_{40/42}$ is a dominent component. Formation of these senile amyloid plaques starts from the cleavage of a transmembrane glycoprotein, amyloid-β protein precursor (AβPP). Once the amyloid protein monomer is produced, it goes through liquid-liquid phase separation from solution phase to particle, small fibril,

mature long fiber, and finally to plaques. The peptide assembly process is directed by hydrogen bonding, Π-Π stacking, hydrophobic, electrostatic, and van der Waals interactions, all leading to stable beta-sheet structures formed with Aβ peptide assemblies.

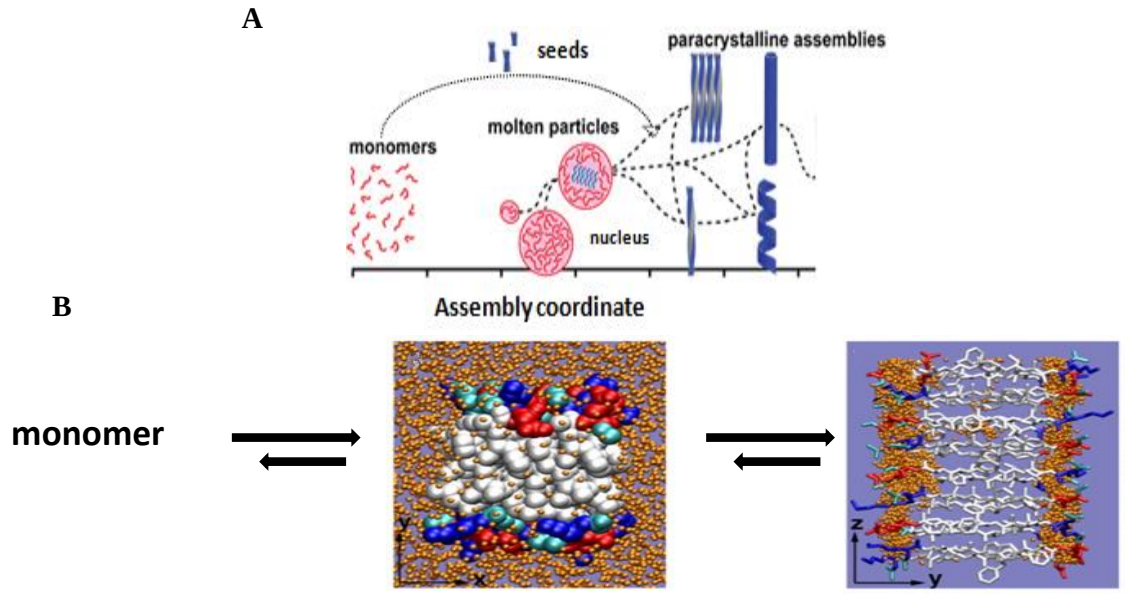

Figure 1-1. Scheme of amyloid protein self-assembly process.

Lipid-amyloid interactions and antimicrobial property of amyloid

The abundance of lipids in brain tissues [30] and the many studies demonstrating that mature amyloid fibrils and plaques colocalize with lipids may correlate with cytotoxicity, which could be a hallmark of the Alzheimer's disease [31,32]. The interaction between amyloid peptides and lipid membrane has been extensively explored [6, 7], showing that negatively charged membrane lipids significantly enhance the aggregation rate of the Aβ-peptide [8-10]. A possible mechanism of membrane-induced amyloid aggregation involves electrostatic interactions, conforming adjustment and a site of condensation for the Aβ-peptide monomers [37]. Interactions between amyloid peptides and lipid membranes include (a)

insertion of amyloid oligomer in lipid membranes and (b) binding and aggregation of amyloid oligomer on surface of lipid membranes, which was shown in **Figure 1-2** [24].

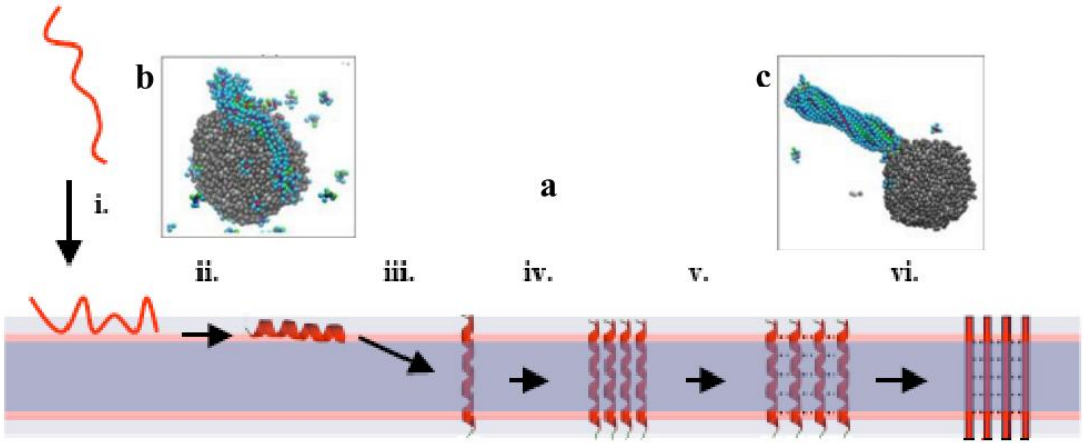

Figure 1-2. Proposed mechanisms of amyloid peptide binding, insertion and aggregation in the presence of lipid membranes [33].

LPS is an endotoxin located on the cell surface of gram-negative bacteria including *E. coli* [11]. As shown in **Figure 1-3**, it contains three regions: a hydrophobic lipid A, a hydrophilic core polysaccharide chain and a hydrophilic O-antigenic polysaccharide side chain [12]. Lipid A, which represents the active center responsible for the endotoxic properties of LPS, can be liberated from LPS by mild acid hydrolysis [13]. Free *E. coli* lipid A consists of a β (1-6)-linked D-glucosamine disaccharide containing two phosphoryl groups with 4 to 7 fatty acid side chains [14, 15]. It has been shown that LPS induces amyloid formation and conformation change of antimicrobial peptide (AMP) such as magainin 2 [16] and HAL-2 [17]. These studies provide evidence that the interaction was mainly caused by the electrostatic interaction between positively charged AMP and negatively charged LPS. Given that Aβ peptides are essentially AMPs [18], it is reasonable to assume that Aβ peptide readily binds and disrupts negatively

charged bacterial lipid membrane, but the direct process is unknown. One hypothesis is nucleation-dependent fibrillization [8] of Aβ peptide induced by LPS containing vesicles, which was supported by a recently reported publication showing the direct binding of the $A\beta_{25-35}$ fibrils to LPS micelles [38]. Another hypothesis is that Aβ peptides induce the leakage of bacterial membrane by insertion, which was proposed by a publication showing that Aβ 1-42 is a membrane-disrupting peptide [19] Further evidence is needed to demonstrate the mechanism and kinetics of this interaction.

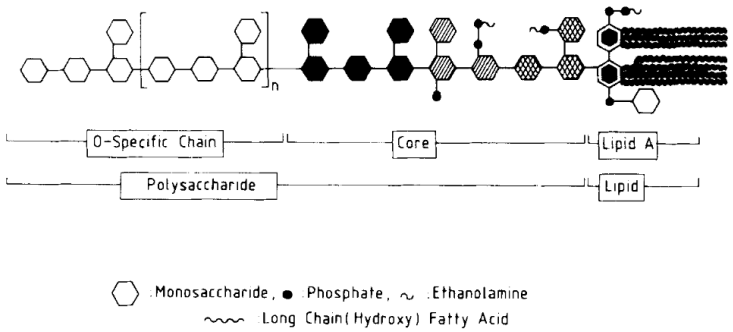

Figure 1-3. Schematic structure of Sulmonelllr lipopolysaccharides [12].

Potential of constructing co-assemblies of amyloid with lipids

Amphiphiles are molecules containing hydrophobic and hydrophilic moieties in the same molecule. Many amphiphilic molecules such as phospholipids and glycolipids self-assemble to generate micelles, rods, ribbons, fiber and nanotubes [20]. As a type of amphiphile, lipid A can also self-assembly to form similar phases in aqueous solution [21]. Peptide amphiphiles (PAs), including amphiphilic peptides and peptides functionalized with alkyl tails, have amyloid-like behavior due to β-sheet formation and electrostatic interaction [22, 23]. With a hydrophilic N-terminus (residues 1 to 28) and a hydrophobic C-terminus (residues 29 to 39 or 29–42), Aβ(1-40/42) is amphiphilic and can self-assembly into various low dimensional crystalline phases [24].

Our group previously reported the self-assembly of peptide/lipid chimers forming fibers, ribbons and tubes [25]. In these cases, Aβ (16-22), $K^{16}LVFFAE^{22}$-NH_2, is linked to alkyl chains from C_2 (N-acetyl) to C_{16} (N-palmitoyl), thus increasing the hydrophobic character of the Aβ peptide. The data established that the cross-β structure can accommodate long acyl chains in the interior of the beta-sheet laminate. Also, a recent published paper constructed the co-assembly of peptide amphiphiles and dodecanoic acid by anion−π interactions with the hypothesis that the alkyl tail of dodecanoic acid bury itself in the hydrophobic core composed of amphiphilic peptides [26]. Another study in Lynn's group [39] explored the ability of Aβ(16-22) homology co-assembling with RNA, based on the discoveries that peptide/nucleic acid interactions are associated with neurodegenerative diseases [25, 27, 28]. Considering the potential of peptides to co-assemble with charged molecules and amphiphiles, lipid A containing both phosphate and alkyl chains [29] have the potential to co-assembly\e with amyloid peptide Aβ(16-22) or Aβ(1-40/42).

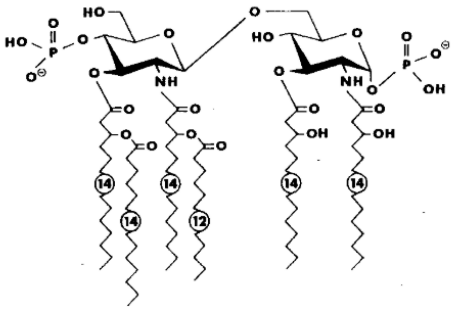

Figure 1-4. Chemical structure of lipid A from *E. coli* J-5 lipopolysaccharide. (Reproduced with permission from Reference 21. Copyright 1985, Wiley)

References

1. Nussbaum, J.M., M.E. Seward, and G.S. Bloom, *Alzheimer disease A tale of two prions.* Prion, 2013. **7**(1): p. 14-19.
2. Lynn, D.G. and S.C. Meredith, *Review: Model peptides and the physicochemical approach to beta-amyloids.* Journal of Structural Biology, 2000. **130**(2-3): p. 153-173.
3. Sampson, T.R., et al., *Gut Microbiota Regulate Motor Deficits and Neuroinflammation in a Model of Parkinson's Disease.* Cell, 2016. **167**(6): p. 1469-+.
4. Branton, W.G., et al., *Brain Microbial Populations in HIV/AIDS: alpha-Proteobacteria Predominate Independent of Host Immune Status.* Plos One, 2013. **8**(1).
5. Zhan, X.H., et al., *Gram-negative bacterial molecules associate with Alzheimer disease pathology.* Neurology, 2016. **87**(22): p. 2324-2332.
6. Terzi, E., G. Holzemann, and J. Seelig, *SELF-ASSOCIATION OF BETA-AMYLOID PEPTIDE(1-40) IN SOLUTION AND BINDING TO LIPID-MEMBRANES.* Journal of Molecular Biology, 1995. **252**(5): p. 633-642.
7. Terzi, E., G. Holzemann, and J. Seelig, *ALZHEIMER BETA-AMYLOID PEPTIDE-25-35 - ELECTROSTATIC INTERACTIONS WITH PHOSPHOLIPID-MEMBRANES.* Biochemistry, 1994. **33**(23): p. 7434-7441.
8. Gorbenko, G.P. and P.K.J. Kinnunen, *The role of lipid-protein interactions in amyloid-type protein fibril formation.* Chemistry and Physics of Lipids, 2006. **141**(1-2): p. 72-82.
9. Hebda, J.A. and A.D. Miranker, *The Interplay of Catalysis and Toxicity by Amyloid Intermediates on Lipid Bilayers: Insights from Type II Diabetes*, in *Annual Review of Biophysics*. 2009. p. 125-152.
10. Domanov, Y.A. and P.K.J. Kinnunen, *Islet amyloid polypeptide forms rigid lipid-protein amyloid fibrils on supported phospholipid bilayers.* Journal of Molecular Biology, 2008. **376**(1): p. 42-54.

11. Raetz, C.R.H. and C. Whitfield, *Lipopolysaccharide endotoxins.* Annual Review of Biochemistry, 2002. **71**: p. 635-700.

12. Luderitz, O., et al., *LIPOPOLYSACCHARIDES OF GRAM-NEGATIVE BACTERIA.* Current Topics in Membranes and Transport, 1982. **17**: p. 79-151.

13. Westphal, O. and O. Luderitz, *CHEMISCHE ERFORSCHUNG VON LIPOPOLYSACCHARIDEN GRAMNEGATIVER BAKTERIEN.* Angewandte Chemie, 1954. **66**(13-1): p. 407-417.

14. Galanos, C., et al., *SYNTHETIC AND NATURAL ESCHERICHIA-COLI FREE LIPID-A EXPRESS IDENTICAL ENDOTOXIC ACTIVITIES.* European Journal of Biochemistry, 1985. **148**(1): p. 1-5.

15. Qureshi, N., et al., *POSITION OF ESTER GROUPS IN THE LIPID-A BACKBONE OF LIPOPOLYSACCHARIDES OBTAINED FROM SALMONELLA-TYPHIMURIUM.* Journal of Biological Chemistry, 1983. **258**(21): p. 2947-2951.

16. Matsuzaki, K., et al., *Interactions of an antimicrobial peptide, magainin 2, with outer and inner membranes of Gram-negative bacteria.* Biochimica Et Biophysica Acta-Biomembranes, 1997. **1327**(1): p. 119-130.

17. Wang, J.R., et al., *Lipopolysaccharide induces amyloid formation of antimicrobial peptide HAL-2.* Biochimica Et Biophysica Acta-Biomembranes, 2014. **1838**(11): p. 2910-2918.

18. Soscia, S.J., et al., *The Alzheimer's Disease-Associated Amyloid beta-Protein Is an Antimicrobial Peptide.* Plos One, 2010. **5**(3).

19. Ambroggio, E.E., et al., *Surface behavior and lipid interaction of Alzheimer beta-amyloid peptide 1-42: A membrane-disrupting peptide.* Biophysical Journal, 2005. **88**(4): p. 2706-2713.

20. Faunce, C.A., et al., *Ordering of lipid A-monophosphate clusters in aqueous solutions.* Journal of Chemical Physics, 2007. **127**(11).

21. Dehsorkhi, A., V. Castelletto, and I.W. Hamley, *Self-assembling amphiphilic peptides.* Journal of Peptide Science, 2014. **20**(7): p. 453-467.

22. Liu, R.T., et al., *Residues 17-20 and 30-35 of beta-amyloid play critical roles in aggregation.* Journal of Neuroscience Research, 2004. **75**(2): p. 162-171.

23. Behanna, H.A., et al., *Coassembly of amphiphiles with opposite peptide polarities into nanofibers.* Journal of the American Chemical Society, 2005. **127**(4): p. 1193-1200.

24. Ni, R., et al., *Remodeling Cross-beta Nanotube Surfaces with Peptide/Lipid Chimeras.* Angewandte Chemie-International Edition, 2012. **51**(27): p. 6635-6638.

25. Lim, L.Z., et al., *ALS-Causing Mutations Significantly Perturb the Self-Assembly and Interaction with Nucleic Acid of the Intrinsically Disordered Prion-Like Domain of TDP-43.* Plos Biology, 2016. **14**(1).

26. Yu, Z.L., et al., *Co-assembly of Peptide Amphiphiles and Lipids into Supramolecular Nanostructures Driven by Anion-pi Interactions.* Journal of the American Chemical Society, 2017. **139**(23): p. 7823-7830.

27. Macedo, B., et al., *Nonspecific Prion Protein-Nucleic Acid Interactions Lead to Different Aggregates and Cytotoxic Species.* Biochemistry, 2012. **51**(27): p. 5402-5413.

28. Marcinkiewicz, M., *beta APP and furin mRNA concentrates in immature senile plaques in the brain of Alzheimer patients.* Journal of Neuropathology and Experimental Neurology, 2002. **61**(9): p. 815-829.

29. Holst, O., et al., *CHEMICAL-STRUCTURE OF THE LIPID-A OF ESCHERICHIA-COLI J-5.* European Journal of Biochemistry, 1993. **214**(3): p. 695-701.

30. Veloso, Antonio, et al. "Distribution of lipids in human brain." Analytical and bioanalytical chemistry 401.1 (2011): 89-101.

31. Kiskis, Juris, et al. "Plaque-associated lipids in Alzheimer's diseased brain tissue visualized by nonlinear microscopy." Scientific reports 5 (2015): 13489.

32. Di Paolo, Gilbert, and Tae-Wan Kim. "Linking lipids to Alzheimer's disease: cholesterol and beyond." Nature Reviews Neuroscience 12.5 (2011): 284.

33. Friedman, R., Pellarin, R., and Caflisch, A. (2009). Amyloid Aggregation on Lipid Bilayers and Its Impact on Membrane Permeability. J Mol Biol 387, 407-415.

34. Selkoe, Dennis J. "The molecular pathology of Alzheimer's disease." Neuron 6.4 (1991): 487-498.

Chapter 2. Exploring the interaction between LPS and amyloid peptide

Introduction

Lipids are used as the basis of cell membranes, therefore being abundant and crucial in both brains and bacteria. Disruption of plasma membrane structure, through the interaction between lipid and amyloid peptide, are associated with neurotoxicity of amyloid in amyloid-related diseases [1]. Lipopolysaccharide (LPS) is the main component of gram-negative bacteria's outer membrane, which has the potential to interact with amyloid if they coexist in the same environment. As a type of antimicrobial peptide [2], Aβ peptide may disrupt the bacterial LPS membrane structure by aggregating on the surface of LPS or inserting into the membrane, because LPS is an endotoxin. To demonstrate the details of this process, in vitro observations and relating measurements are needed.

According to Annalia Asti's results published in 2017 (3), in vitro interaction of Aβ(25-35) fibrils with LPS particles were shown with TEM, indicating a direct affinity of LPS and Aβ(25-35) at the molecular level. However, the author did not reveal the structure change of Aβ(25-35) with other useful methods, and failed to explain why they chose Aβ(25-35) truncation to study Aβ fibrillogenesis.

Here, combining TEM, CD and ATR-IR, we characterized and monitored the interaction between LPS and Aβ(16-22)/Aβ(1-40), especially demonstrated the change of amyloid's secondary structure. The

results indicate the ability of LPS to promote amyloid peptide aggregation, suggesting the importance of bacterial components in the pathogenesis of Alzheimer's disease.

Methods

Peptide synthesis and purification: Peptides were synthesized on a Liberty CEM Microwave Automated Peptide Synthesizer (NC, USA) utilizing a FMOC-Rink Amide MBHA Resin (AnaSpec, CA, USA). All FMOC protected amino acids were purchased from Anaspec, and remaining chemicals from Sigma-Aldrich. Each peptide synthesis was performed at 0.1 mmol using a 30 mL reaction vessel at a scale of 0.1mmol. FMOC-Rink Amide MBHA Resin was initially swollen using ~7 mL dimethylformamide for 15 minutes. FMOC deprotection was achieved by addition of 20% piperdine 0.1M N-Hydroxybenzotriazole (HOBt) in dimethylformamide with microwave power set to maintain temperature between 45-55°C for 180 sec, followed by 3X flushing with dimethylformamide. Each coupling step was performed using 0.1M FMOC protected amino acid, and activated with 0.1 M 2 - (1H - Benzotriazole - 1 - yl) - 1,1,3,3 - tetramethyluronium hexafluorophosphate (HBTU), and 0.2M N,N – Diisopropylethylamine (DIEA) in DMF. Coupling temperatures were maintained between 75-82°C by optimizing microwave power for 300 sec. After coupling, the resin was rinsed with three aliquots of dimethylformamide. At the end of coupling steps, 20% acetic anhydride in dimethylformamide was added to acetylate the N terminus of the peptides. The capping reaction was allowed to proceed for 3 hours at room temperature. Resin was filtered and washed with dichloromethane and allowed to air dry. Peptides were cleaved from the resin using trifluoroacetic acid/thioanisole/1,2ethanedithiol/anisole (90: 5 : 3 : 2, v/v/v/v) at room temperature for 3 hrs. The cleaved peptide TFA solution was filtered and precipitated by dropwise addition of cold (-20°C) diethyl ether. Precipitated product was centrifuged at 3000 rpm for 3 min, and the pellet was subjected to 3 additional rounds of washing with cold diethyl ether. Precipitated product was desiccated overnight.

Dried peptides were dissolved in minimal volume of 40% acetonitrile + 0.1% trifluoroacetic acid and purified by RP-HPLC using a C18-reverse phase column with an acetonitrile-water gradient. Samples eluted from HPLC (10μL) were mixed with 2,5dihydroxybenzoic acid matrix (10 μL), 3x2 μL drops were placed on individual spots of MALDI plate and allow to dry in dessicator, and MALDI subsequently confirmed the molecular weight of each peptide used.

Peptide Assembly: Lyophilized Aβ(16-22) peptide was dissolved in 1,1,1,3,3,3-hexafluoro-2-propanol (HFIP, Sigma) and sonicated for 30 min, then dried in the centrivap at 40 ℃, 2000 rpm for 20min. The resultant clear film was dissolved in 40% acetonitrile/water (with or without 0.1 vol% TFA), bath sonicated for at least 10 min and, unless indicated, incubated at room temperature for assembly. To produce unassembled Aβ(16-22) peptide, lyophilized Aβ(16-22) peptide was dissolved in 1,1,1,3,3,3-hexafluoro-2-propanol (HFIP, Sigma) and sonicated for 30 min and stored at room temperature in HFIP. For Aβ(1-40), Aβ was dissolved in 10% w/v NH_4OH to a concentration of 0.5 mg/ml in a glass vial. After a 10 min incubation on the bench at room temperature, the glass vial was bath-sonicated for 5 min. The solution was then divided into 1 ml aliquots in 1.5 ml Eppendorf tubes before they were flash-frozen in liquid nitrogen and lyophilized. To assembly Aβ(1-40) in phosphate buffer, the NH_4OH-treated peptide was dissolved in 1 mM NaOH (pH ~ 10.8, 90% of the volume to make a 100 μM solution) until the solution was visibly clear of white powder, before 10X sodium phosphate buffer with 0.2% NaN_3, pH 7.1 (the remaining 10% volume) was added, bringing the final concentration to 100 μM Aβ in 10 mM sodium phosphate with 0.02% NaN_3 at pH 7.4. Finally, large aggregates were removed by filtration through a pre-rinsed 0.22 μm filter before the sample was ready for use.

LPS assembly and LPS-Aβ incubation: LPS powder was weighted in the vial, and dissolved directly in HPLC grade water, vortexed and sonicated until solution becomes clear. For co-assembly, Aβ solution and LPS solution were mixed in certain ratio and incubated at room temperature or 37℃.

Transmission Electron Microscopy (TEM): A TEM copper grid with a 200 mesh carbon Support (Electron Microscopy Sciences) was covered with 10 μL of a diluted peptide solution (0.05 mM to 0.1 mM) for 1 min before wicking the excess solution with filter paper. 10 μL of the staining solution (2% uranyl acetate, Sigma-Aldrich or methylamine tungstate, Ted Pella, Inc) was added and incubated for 2 min, excess solution was wicked away, and the grids were placed in desiccators to dry under vacuum overnight.

Circular Dichroism spectroscopy: Jasco-810 circular dichroism (CD) spectropolarimeter was used to record CD spectra in a 20 μL cell with a 0.1 mm path length at room temperature. The reported spectra represent the average of three scans between 260 nm to 190 nm with a stepsize of 0.2 nm and a speed of 100 nm/s. Ellipticity , θ, in mdeg was converted to Molar ellipticity [θ] with $[\theta] = \theta/(10 \times c \times l)$, where c is the peptide concentration in moles/L and l is the path length in cm.

Attenuated Total Reflectance Fourier Transform Infrared (AT-FTIR): Aliquots (10μL) of peptide solution were dried as thin films on an Pike GaldiATR (Madison, WI, USA) ATR diamond crystal. FT-IR spectra were acquired using a Jasco FT-IR 4100 (Easton, MD, USA) at room temperature and averaging 500 to 800 scans with 2 cm^{-1} resolution, using either an MCT or TGS detector, 5mm aperture and a scanning speed of 4mm/sec. Spectra were processed with zero-filling and a cosine apodization function. IE-IR spectra were normalized to the peak height of the ^{12}C band.

Results

Characterizing the interaction between Aβ(16-22) peptide and LPS

To directly demonstrate the interaction of Aβ peptide with LPS, Aβ (16-22) peptide was incubated with LPS solution of fibers and particles at pH 7 in pure water. After incubating for different days, TEM was utilized to characterize their interaction. However, the TEM images of **Figure 2-1** didn't define the colocalization of LPS and peptide, however, they supported the amyloid fibrils were surrounded by LPS. This may be explained by the complicated structure of LPS, which makes it difficult to co-assemble with Aβ peptides. Further experiments need to be designed to confirm the role of LPS in promoting Aβ (16-22) fibrillization and aggregation.

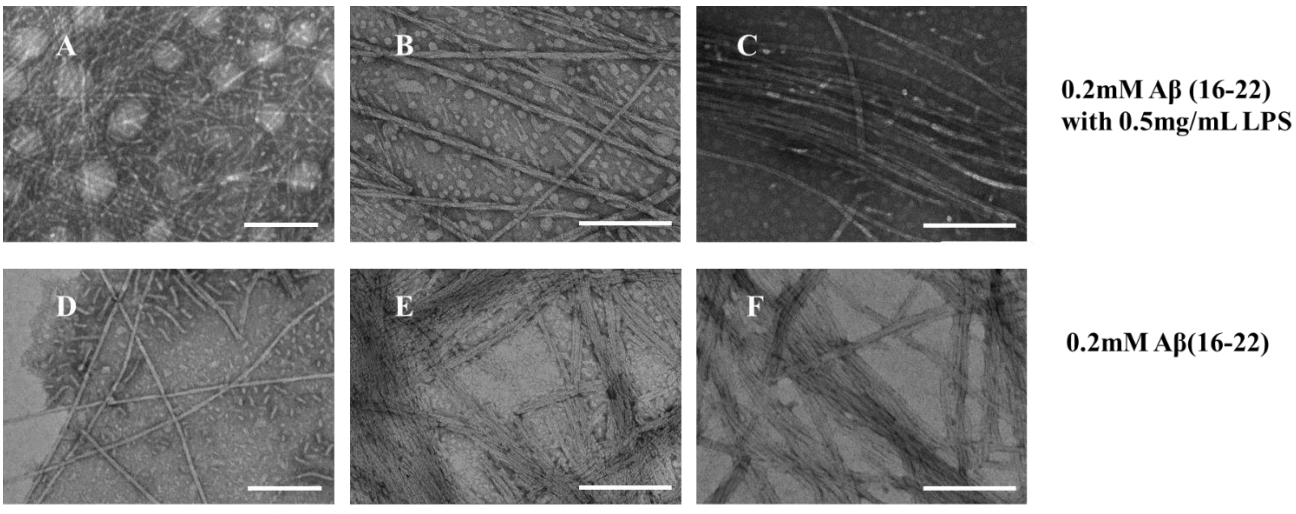

Figure 2-1. TEM images of 0.2mM Aβ (16-22) with 0.5mg/mL LPS in water of pH 7 at room temperature after 1 day (A), 2 weeks (B) and 3 weeks (C); self-assembly of peptide at the same condition (D, E, F).

CD and FT-IR are two powerful techniques to characterize the peptide secondary structure. For Aβ peptides, typical absorption in CD spectra and peaks in IR spectra suggest β-sheet structures.

To analyze the secondary structure of Aβ(16-22) in the absence and presence of LPS, CD spectra were collected at different incubation time (1, 2, 4, 7 days) and concentration of LPS (0, 0.1 0.5, 1.0 mg/mL). CD spectra of 0.2mM peptide self-assembly did not show obvious secondary structure, suggesting little aggregation of Aβ(16-22) at such low concentration. The negative ellipticity at 215 nm increased, consistent with the secondary structure of Aβ(16-22) peptide changing from unordered to β-sheet. **Figure 2-2** shows that either the concentration of LPS or the incubation time increases, the ellipticity at 215 nm increases. These results confirmed the role of LPS in inducing the aggregation of amyloid because β-sheet structure is the indicator of amyloid assemblies (4). To further determine whether the aggregation mainly induced by the negatively-charged phosphates on LPS, we compared the CD spectra between Aβ(16-22) in the 20mM phosphate buffer solution (PBS) with the spectra of Aβ (16-22) in the aqueous of LPS. **Figure 2-3** shows that there was no obvious β-sheet formation in the PBS, which indicated that the electrostatic interaction may not be the determined factor inducing the Aβ peptide aggregation.

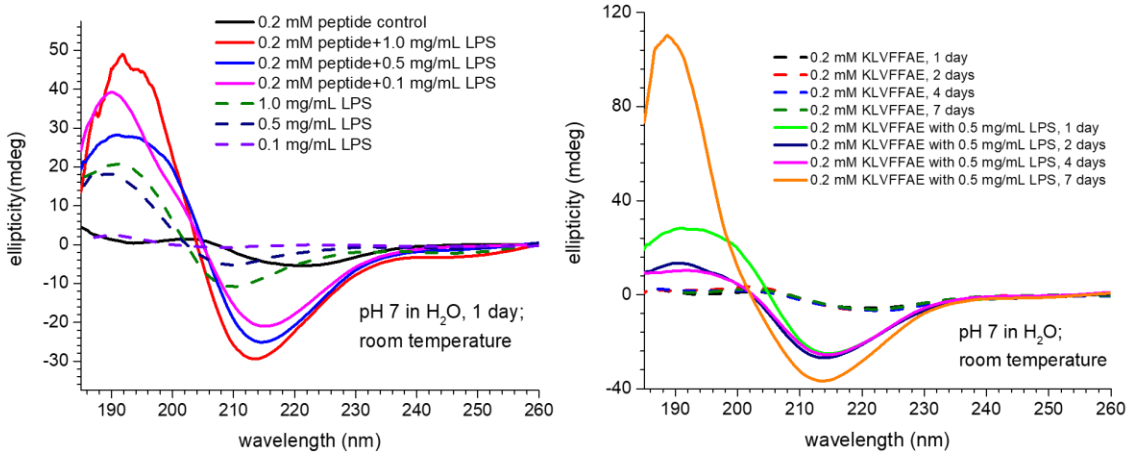

Figure 2-2 CD spectra of (A) 0.2mM Aβ(16-22) in the presence of different concentration of LPS; (B) 0.2mM Aβ(16-22) in the presence of 0.5mg/mL LPS at different days.

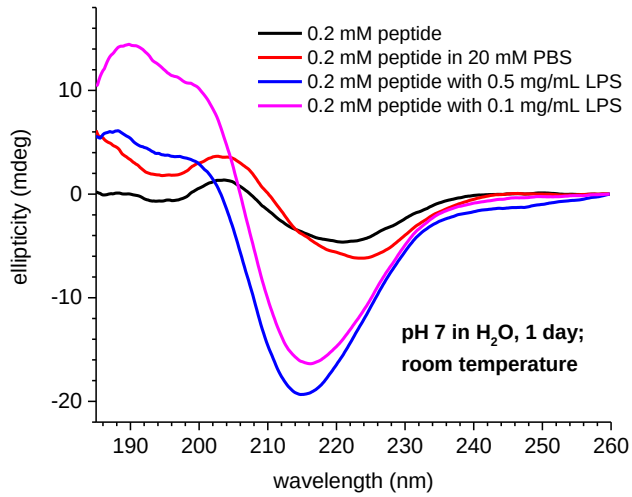

Figure 2-3 CD spectra of 0.2mM Aβ(16-22) in the absence and presence of LPS or PBS.

From CD spectra, we could conclude that the existence of LPS improve the β-sheet formation of Aβ(16-22), but more detailed information of amyloid's secondary registry should be provided by FT-IR spectra. ATR-FTIR spectra were obtained from 0.2mM Aβ(16-22) and 0.5mg-mL LPS assembly after 1day and 4days. From **Figure 2-4**, the absorption at 1624cm^{-1} in the spectra of LPS-Aβ(16-22) assembly in the Amide I region showed the formation of β-sheet structure, consistent with CD results. Also, the 1694cm^{-1} side peak suggested anti-parallel registry taken by Aβ(16-22) with or without LPS. However, the spectra of LPS-Aβ(16-22) assembly may be just the overlap of the spectra of LPS and Aβ(16-22) self-assembly, which cannot indicate the interaction between LPS and peptide. Thus, ATR-FTIR may not be a suitable method to characterize the interaction pattern in LPS-Aβ (16-22) assemblies.

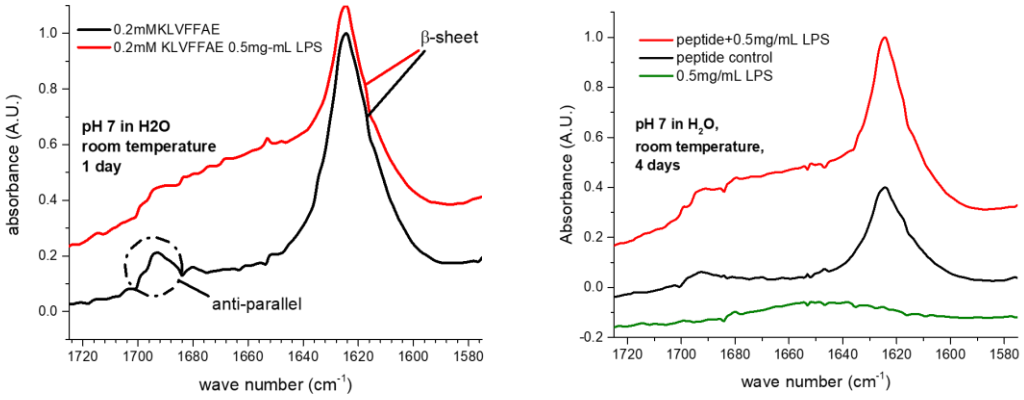

Figure 2-4 ATR-IR spectra of LPS-Aβ (16-22) assembly.

Time-dependent interaction of Aβ(1-40) and LPS

To explore whether LPS induces the assembly of Aβ(1-40), low concentration of Aβ(1-40) solution of 0.2mg-mL was incubated with 0.5mg-mL LPS at 37 ℃, and monitored by TEM. The images showed that without incubated with LPS, 0.2mg-mL Aβ(1-40) was not able to form fibrils; however, Aβ(1-40) forms long peptide fibrils gradually in the presence of LPS. Though it is not clear how LPS interacted with Aβ(1-40), it induces the time-dependent aggregation of Aβ(1-40).

CD spectra of Aβ(1-40)-LPS assemblies were also taken after 5 days. However, there is no obvious absorption in the spectra, which can be seen as noise.

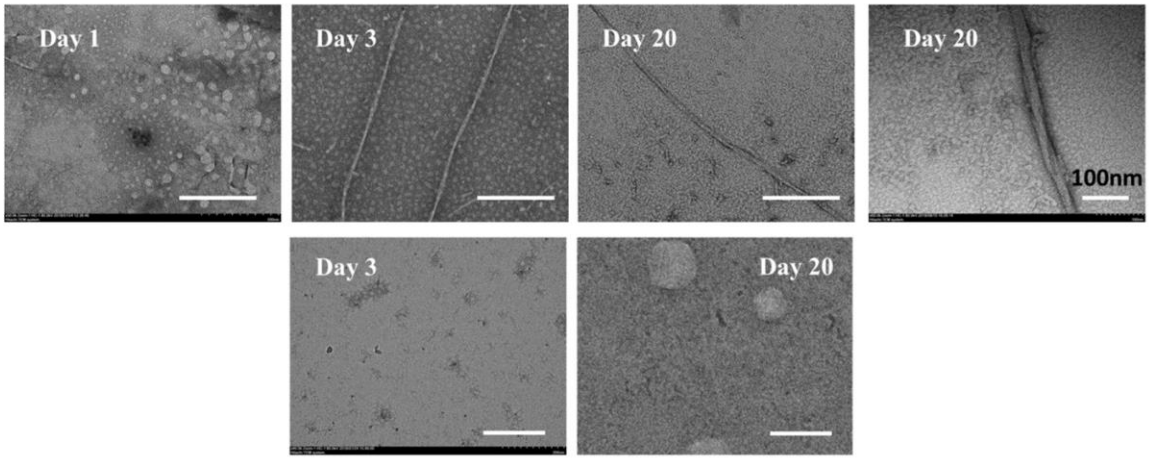

Figure 2-5. TEM images of Aβ(1-40)-LPS assembly (fist line) and Aβ(1-40) self-assembly (second line). Scale bar = 200nm.

Conclusion

In this chapter, LPS-induced aggregation process of Aβ(16-22) and Aβ(1-40) was demonstrated with TEM images and CD spectra. At a low concentration, Aβ peptide is difficult to conduct phase transitions; but LPS accelerates this process, though the mechanism has not been identified from our data.

References

(1) Demuro, A., Mina, E., Kayed, R., Milton, S. C., Parker, I., and Glabe, C. G. (2005). Calcium dysregulation and membrane disruption as a ubiquitous neurotoxic mechanism of soluble amyloid oligomers. Journal of Biological Chemistry 280, 17294-17300.

() Soscia, S.J., et al., *The Alzheimer's Disease-Associated Amyloid beta-Protein Is an Antimicrobial Peptide.* Plos One, 2010. **5**(3).

(3) Asti A. Bacterial Lipopolysaccharide (LPS) and Alzheimer's Disease[J]. Handbook of Infection and Alzheimer's Disease, 2017, 5: 383.

(4) Childers, W.S., et al., *Phase Networks of Cross-beta Peptide Assemblies.* Langmuir, 2012. **28**(15): p. 6386-6395.

Chapter 3. Defining the structure of lipid A-amyloid assembly

Introduction

Last chapter studies the interaction between LPS and amyloid, confirming that LPS plays a role in inducing amyloid aggregation. However, we failed to construct homogeneous LPS-amyloid assembly. LPS does not have exact chemical formula and consists of three regions, including lipid A, "core" oligosaccharide, and a distal polysaccharide (1). As a result, it is difficult to analyze the interaction between LPS and amyloid as well as revealing the structure of their assemblies.

Lipid A is the endotoxin part of LPS which constructs bacterial outer membrane. Moreover, it has fixed chemical formula so that it can be used as a substitute for LPS to analyze the structure of bacterial lipid-amyloid assemblies. Lipid A contains both hydrophilic saccharides and phosphates, which may have electrostatic effect with positively charged residues of amyloid peptides, and hydrophobic alkyl chains, which may insert into amyloid's hydrophobic laminations. Based on these possible interaction, two models of lipid A-amyloid were proposed, as shown in **Figure 3-1**. These two models can be differentiated by XRD because peptide β-sheet lamination distance will be enlarged in the first model when lipid A's alkyl chains insert into the laminations (2). First of all, we need to construct homogeneous assemblies in vitro and characterize their structures.

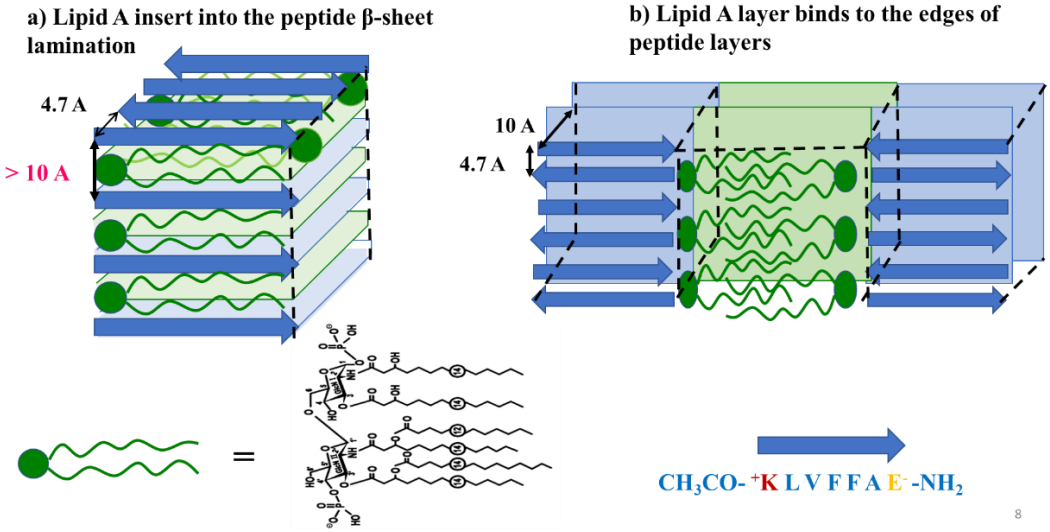

Figure 3-1. Two proposed models of lipid A/Aβ (16-22) co-assemblies.

Methods

Lipid A assembly

Lipid A powder (from *Escherichia coli* F583 (Rd mutant)) was dissolved in $CHCl_3$/MeOH (1:1, v/v) mixture first, then distributed in vials and dried with nitrogen gas. After that lipid A was re-dissolved in aqueous solution and sonicated overnight until forming transparent and clear solution. Lipid A solution was incubated with amyloid peptide solution or self-assembled.

Results

TEM images of Aβ(16-22)-lipid A co-assemblies

To explore if lipid A can co-assemble with Aβ(16-22), we tried to construct their co-assemblies in different solution and observed their morphology by taking TEM images at different days. **Figure 3-2** and **3-3** showed the images of co-assemblies in pure water and 40% ACN, respectively. In water, the morphologies of lipid A-Aβ(16-22) co-assemblies are not stable or homogeneous, but they differed significantly from lipid control and peptide control. In 40% ACN, the morphologies of the co-assemblies are homogeneous wide sheets or ribbons combined with small particles. Compared to the images of lipid A, which showed particles, and images of Aβ(16-22) which showed long fibers, the growth of lipid A-Aβ(16-22) assemblies may be explained by nucleation-dependent fibrillization of peptide in the presence of phospholipid nucleus (3). Based on our previous knowledge, Aβ(16-22) peptide is the nucleation core of the Aβ peptide and it follows 2-step nucleation mechanism that amyloid fiber grows from the metastable particle phase (4). Lipid A particles provide hydrophobic environment for Aβ monomers aggregating and elongation, thus inducing the assemble of peptide with lipid.

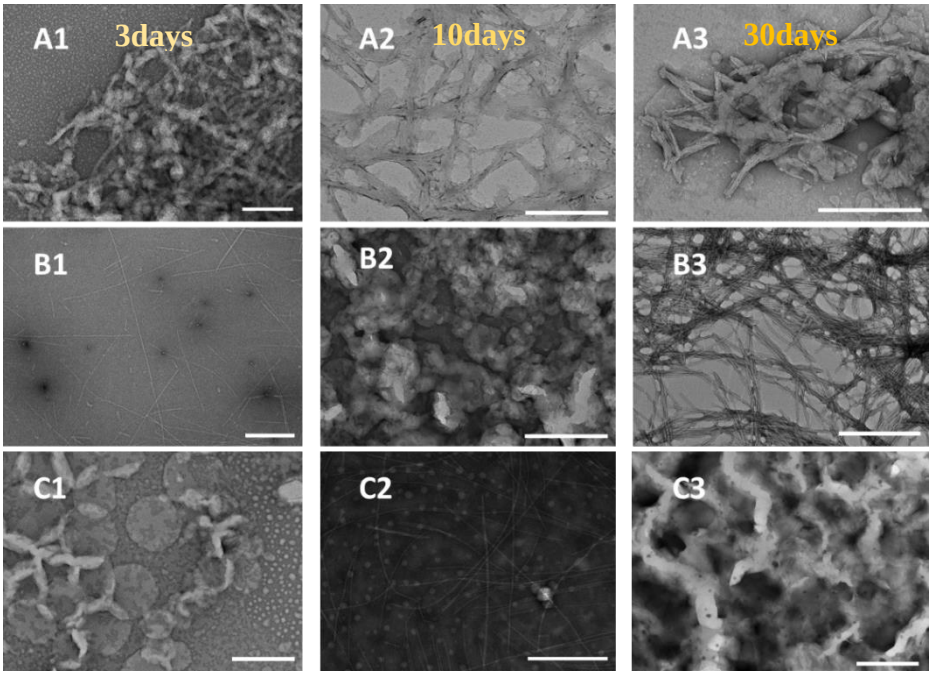

Figure 3-2 Assembled 0.2mM lipid A with 0.2mM KLVFFAE in pure H_2O after 3 days (A1, B1, C1), 10 days (A2, B2, C2) and 30 days (A3, B3, C3);

TEM images of co-assemblies (A1-A3); Self-assembly of peptide(B1-B3); self-assembly of lipid A(C1-C3); scale bar=500nm.

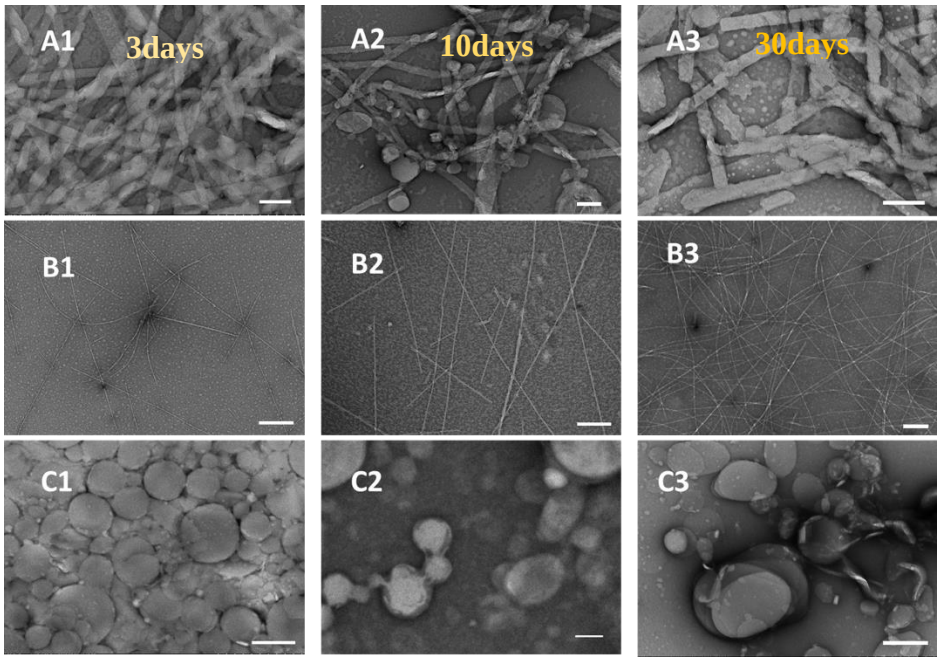

Figure 3-3 Assemble 0.2mM lipid A with 0.2mM KLVFFAE in 40% ACN after 3 days (A1, B1, C1), 10 days (A2, B2, C2) and 30 days (A3, B3, C3); TEM images of Co-assembly (A1-A3); Self-assembly of peptide (B1-B3); Self-assembly of lipid A (C1-C3); scale bar = 200nm.

pH-dependent co-assembly process

There are two possible interaction mainly existed in lipid A-Aβ(16-22) co-assemblies: electrostatic interaction and hydrophobic effect. Does the electrostatic interaction between negatively charged lipid A and positively charged lysine residue on Aβ(16-22) contribute to co-assembly? To examine this hypothesis, 0.1 mM lipid A and 0.2 mM KLVFFAE were incubated in 40% ACN at pH 2 (containing 0.1% TFA) and pH 7 (no TFA), respectively. Charges and electrostatic interaction of lipid A and amyloid at different pH were listed in **Table 3-1**.

TEM images of lipid A and Aβ(16-22) co-assembly at pH 2 and pH 7 were taken after 4 days and 20 days. Images of 4 days showed that at pH 2, only tiny peptide fibrils were observed due to no electrostatic interaction between lipid and peptide while at pH 7, lipid improved the bundling of peptide fibrils since there is electrostatic interaction. As a result, electrostatic interaction influenced the morphology of lipid A-Aβ(16-22) co-assemblies and accelerate the co-assembly process. However, after 20 days, there was no obvious difference between the co-assembly structures at different pH. These results indicated that though the pH-related electrostatic effect influenced the kinetic intermediate of lipid A-Aβ(16-22) co-assemblies, final stable structure is determined by hydrogen bonding and hydrophobic effect.

pH	charge of lipid A	charge of Aβ(16-22)	prediction of interaction
2	0	+1 on Lys	No electrostatic interaction
7	-1 on per phosphate	+1 on Lys and -1 on Glu	Electrostatic interaction between phosphate and both Lys and Glu

Table 3-1. Prediction of charges and interaction between lipid A and Aβ(16-22) at different pH.

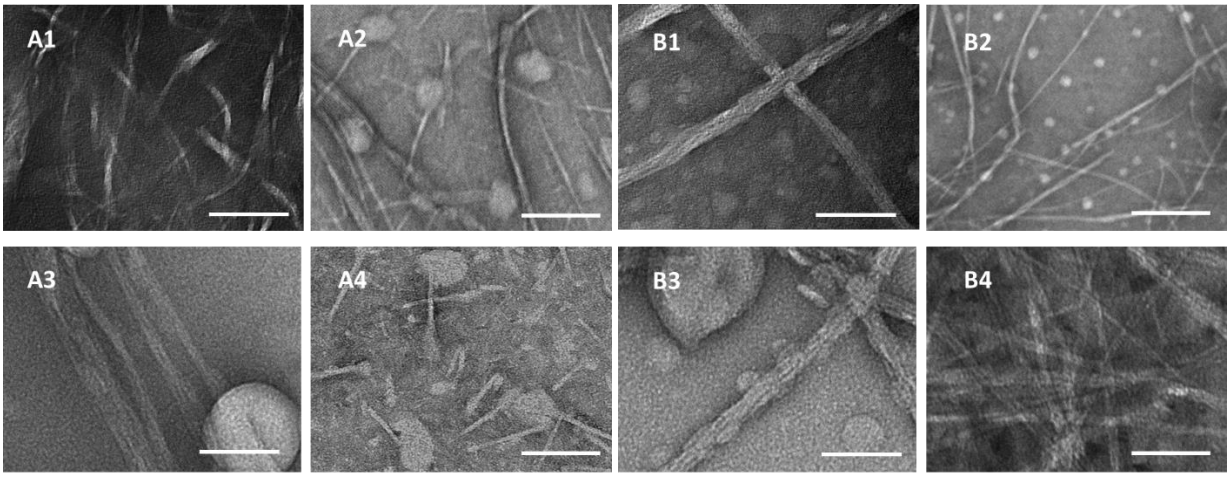

Figure 3-4. Incubate 0.2mM Aβ(16-22) with 0.1mM lipid A at different pH in 40% ACN after 4 days (first line) and 20 days (second line); A1-A4 were incubated at pH 2 and B1-B4 were incubated at pH 7. A2, A4, B2, B4 are Aβ(16-22) self-assembly controls. Scale bar = 100nm.

ATR-FTIR measurement of lipid A-Aβ (16-22) co-assemblies

ATR-FTIR has been used to analyze the structure of peptides or proteins in lipid membranes (5). For lipid A, IR spectra showed the CH_2/CH_3 antisymmetric stretch and symmetric stretch at 2920 cm^{-1} and 2850 cm^{-1} as well as the carbonyl absorption at 1730 cm^{-1}. For peptides, the most important information provided by IR is the Amide I band correlating with the secondary structures. The IR results are consistent with β-sheet absorption at 1625 cm^{-1} in both lipid A-Aβ(16-22) co-assemblies and mixture of lipid A/Aβ(16-22) controls, but the β-sheet absorption is much higher in the co-assemblies. Since ATR-IR is not a quantitative method, it is only credible to compare the ratio between absorptions of different peaks. The wave number of carbonyl absorption did not change in the lipid A-Aβ(16-22) co-assemblies compared to lipid A/Aβ(16-22) controls, which means that there may not be hydrogen bonding between lipid A alkyl chains and Aβ (16-22) peptide backbones.

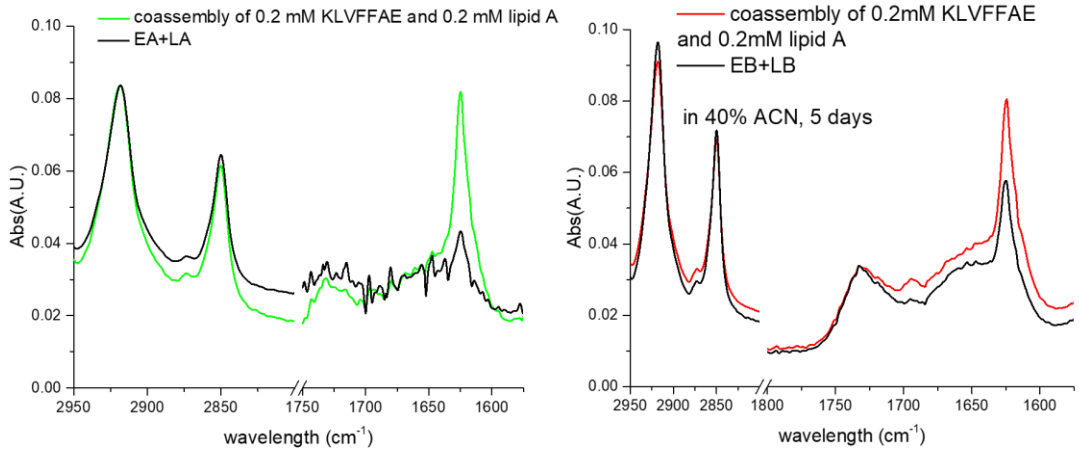

Figure 3-5. ATR-IR spectra of lipid A-Aβ (16-22) co-assembly.

Conclusion

In this chapter, we constructed the co-assemblies of lipid A/Aβ(16-22) in both aqueous and organic solutions. Their structures were characterized with TEM and ATR-FTIR, showing the potential of lipid A-Aβ(16-22) co-assembly as a model to study the interaction between LPS and Aβ(1-40/42). The experimental results indicated that both electrostatic and hydrophobic effect contribute to interaction between lipid A and Aβ(16-22), but there is no direct hydrogen bonding between their carbonyl groups and lipid A did not influence the secondary structure of amyloid. So it is hard to define the accurate structure of lipid A/Aβ(16-22) assemblies without further experiments, but according to FTIR spectra, the second model in which lipid A layer binds to the edges of amyloid layer is preferred.

Perspectives

Define the structure of lipid A/Aβ (16-22) assemblies

From the results of FTIR and CD, it is hard to define β-sheet registry of lipid A/Aβ (16-22) assemblies, which could be obtained from isotope-edited FTIR and $^{13}C\{^{15}N\}$ REDOR and ^{13}C DQF-DRAWS solid-state NMR (see **Figure 5-4**). Considering the chemical structure and properties of lipid A and Aβ (16-22), there are two possible models of lipid A/Aβ (16-22) co-assembly shown in **Figure 3-1**. Model a hypothesizes that lipid A can insert into the laminations of peptide β-sheets, so the d spacing of β-sheet lamination will be wider than the d spacing without lipid A insertion. This can be examined by X-ray diffraction. **Figure 5-1** gives an example of how diffraction of N-acyl-Aβ (16-22) peptide assemblies

enlarges from 9.8 A to 11.5 A after the C_{12} alkyl chain inserts into the lamination of N-acetyl-Aβ (16-22). In contrast, if lipid A binds to the edges of peptide layers, as shown in model b, then the d spacing of β-sheet lamination will not change. Also, multilayers are expected to form in model b, which can be characterized by TEM images, EFM mapping and confocal fluorescence to show the merging of lipid A and Aβ (16-22) layers. To further analyze the interaction between peptide backbones and lipid A headgroups, the distance between ^{13}C enrichment of the carbonyl of leucine or the N-terminal acetate and lipid A phosphate headgroups can be assigned in $^{13}C\{^{31}P\}$ REDOR (see **Figure 5-5**).

Extend the lipid A-Aβ (16-22) interaction to the LPS-Aβ (1-40/42) and bacterial membrane-Aβ (1-40/42) interaction

With the structure and interacting mechanism of lipid A-Aβ (16-22) co-assembly, I will extend this model to the interactions between LPS and Aβ (1-40/42) or even bacterial membrane and Aβ (1-40/42). However, the structure of LPS and bacterial membrane is much more complicated than lipid A, so perhaps similar results of diffraction and ssNMR will not be clear. In that case, I will consider using fluorescence to visualize the direct binding or inserting of Aβ peptides to LPS membrane. I will also evaluate any correlation between the morphology of Aβ peptides, monomer, fibril or plaque, induced by the disruption of the bacterial membrane.

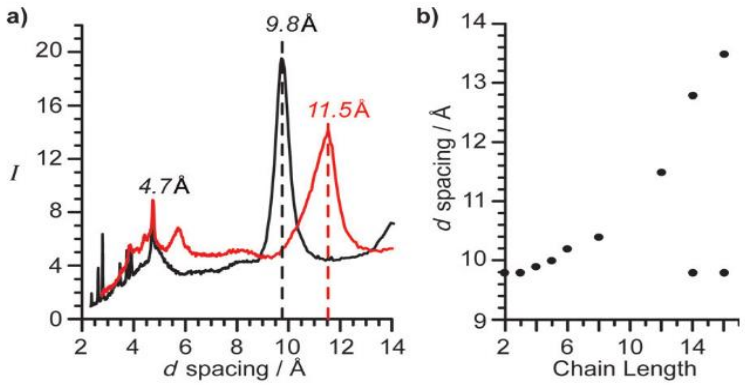

Figure 5-1. Powder and oriented electron diffraction of N-acyl-Aβ (16-22) peptide assemblies. a) X-ray powder diffraction of N-lauroyl-Aβ (16-22) (red) and and N-acetyl-Aβ (16-22) tubes (black) [1].

(1) Electrostatic Force Microscopy (EFM): In the EFM amplitude micrographs, positively charged surfaces are white and negatively charged surfaces are dark, thus mapping the charge distribution on the surface of lipid/peptide co-assembly and revealing the distribution pattern of lipid and peptide.

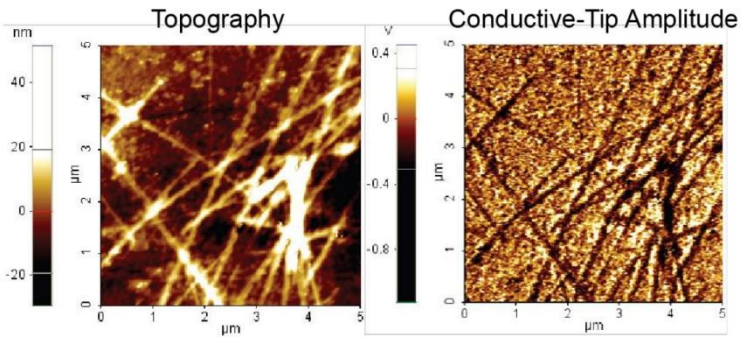

Figure 5-2. Atomic and electrostatic force microscopy images of (K16pY) (E22L) nanotube assemblies with surfaces coated by the positively charged protein. (**Left**) topography images of peptide nanotubes and (**Right**) EFM amplitude micrographs with a DC bias = +1V [2].

(2) Isotope-edited FTIR Spectra: The distribution between ^{12}C and ^{13}C bands in FTIR spectra reflects the extent of the packing along the entire β-sheets, which are diagnostic of the β-strand orientation and registry differences between lipid/peptide co-assembly and peptide self-assembly.

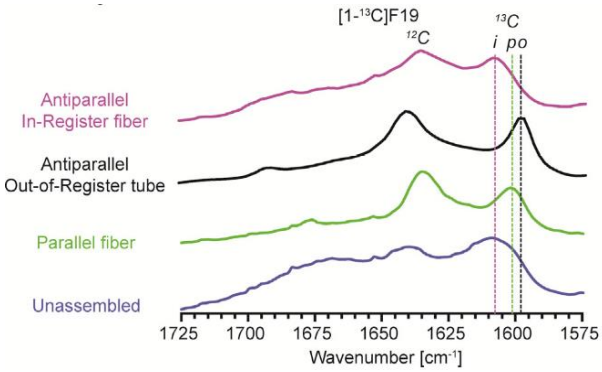

Figure 5-3. IE-IR spectra of mature, homogenous [1-^{13}C] F19 enriched peptides in antiparallel in-register (magenta), antiparallel out-of-register (black), and parallel [^{13}C] (green) strand orientations and unassembled (blue) peptide [3].

(3) Solid state NMR: Peptide registry in amyloid assemblies have been assigned definitively by ssNMR analyses and shown to correlate with isotope edited (IE) FT-IR analyses.

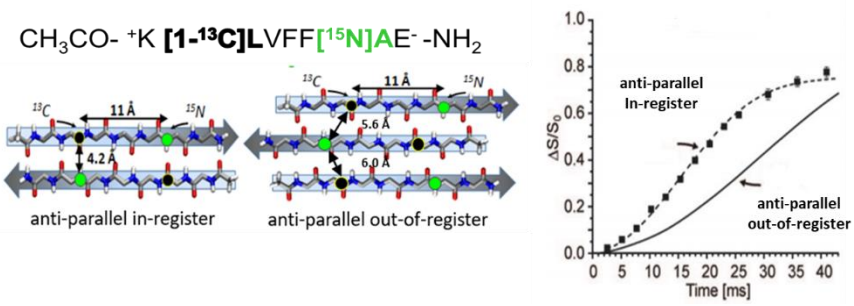

Figure 5-4. $^{13}C\{^{15}N\}$ REDOR and ^{13}C DQF-DRAWS solid-state NMR correlate with IR and showing the β-sheet register information [3].

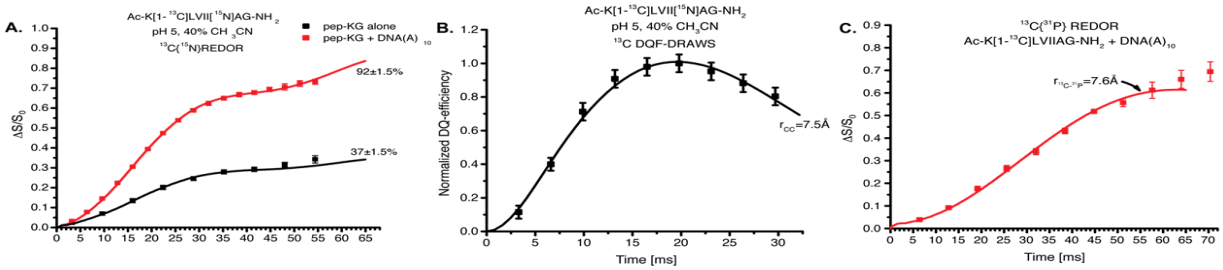

Figure 5-5. Structural characterization of DNA/Peptide co-assemblies. (A) $^{13}C\{^{15}N\}$ REDOR (B)^{13}C DQF-DRAWS (C) $^{13}C\{^{31}P\}$ REDOR [5].

(4) Confocal Fluorescence: ThT is a defining probe for β-sheet peptide assemblies as it displays increased fluorescence and a characteristic red shift of its emission spectrum upon binding to those assemblies [5]. With ThT fluorescence, the β-sheet structures in lipid/peptide assemblies are observed. With confocal fluorescence, merging of LPS and Aβ peptides are showed, thus proving the colocalization.

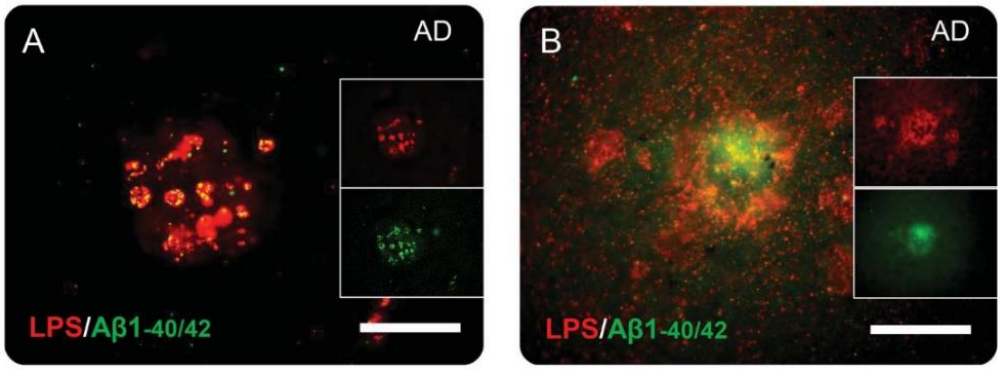

Figure 5-6. Association of lipopolysaccharide (LPS) with amyloid plaques in Alzheimer disease (AD) brains [6].

Reference

1. Ni, R., et al., *Remodeling Cross-beta Nanotube Surfaces with Peptide/Lipid Chimeras.* Angewandte Chemie-International Edition, 2012. **51**(27): p. 6635-6638.

2. Lu, K., et al., *Exploiting amyloid fibril lamination for nanotube self-assembly.* Journal of the American Chemical Society, 2003. **125**(21): p. 6391-6393.

3. Gawrisch, K. and B.W. Koenig, *Lipid-peptide interaction investigated by NMR.* Peptide-Lipid Interactions, 2002. **52**: p. 163-190.

4. Allisandra K. Rha, Dibyendu Das, Anil K. Mehta, Olga Taran, Yongang Ke, David G. Lynn, 2017. Structural insights on ribonucleoprotein (RNP) granule maturation and disease etiology (in progress)

5. Terzi, E., G. Holzemann, and J. Seelig, *Interaction of Alzheimer beta-amyloid peptide(1-40) with lipid membranes.* Biochemistry, 1997. **36**(48): p. 14845-14852.

6. Zhan, X.H., et al., *Gram-negative bacterial molecules associate with Alzheimer disease pathology.* Neurology, 2016. **87**(22): p. 2324-2332.

References

(1) Raetz, C.R.H. and C. Whitfield, *Lipopolysaccharide endotoxins.* Annual Review of Biochemistry, 2002. **71**: p. 635-700.

(2) Ni, R., et al., *Remodeling Cross-beta Nanotube Surfaces with Peptide/Lipid Chimeras.* Angewandte Chemie-International Edition, 2012. **51**(27): p. 6635-6638.

(3) Necula, M., C.N. Chirita, and J. Kuret, *Rapid anionic micelle-mediated alpha-synuclein fibrillization in vitro.* J Biol Chem, 2003. **278**(47): p. 46674-80.

(4) Hsieh, M.C., D.G. Lynn, and M.A. Grover, *Kinetic Model for Two-Step Nucleation of Peptide Assembly*. Journal of Physical Chemistry B, 2017. **121**(31): p. 7401-7411.

(5) Tamm, L.K. and S.A. Tatulian, *Infrared spectroscopy of proteins and peptides in lipid bilayers.* Quarterly Reviews of Biophysics, 1997. **30**(4): p. 365-429.

Chapter 4. Constructing other lipid-amyloid assembly

Introduction

In the last chapter, we showed that lipid A could co-assemble with amyloid peptide. However, lipid A is not a perfect model lipid to study amyloid-membrane interaction because of its low solubility in aqueous solution and complicated structure. It is better to replace lipid A with a kind of membrane lipid which is abundant in brains and has similar reacting properties as lipid A.

To satisfy these requirements, phosphatidylinositol (PI) was chosen as a susbsitiute of lipid A. As a kind of ganglioside, PI contributes to up to 10% of phospholipids in brain tissue (1). Moreover, **Figure 4-1** demonstrated the similarity in the structure of PI and lipid A. Since they both contain long fatty chains and phosphate ion, PI may perform similar properties.

After the substitute phopholipid was determined, PI was incubated together with Aβ(16-22) in 40% ACN. TEM images of samples were taken continuously.

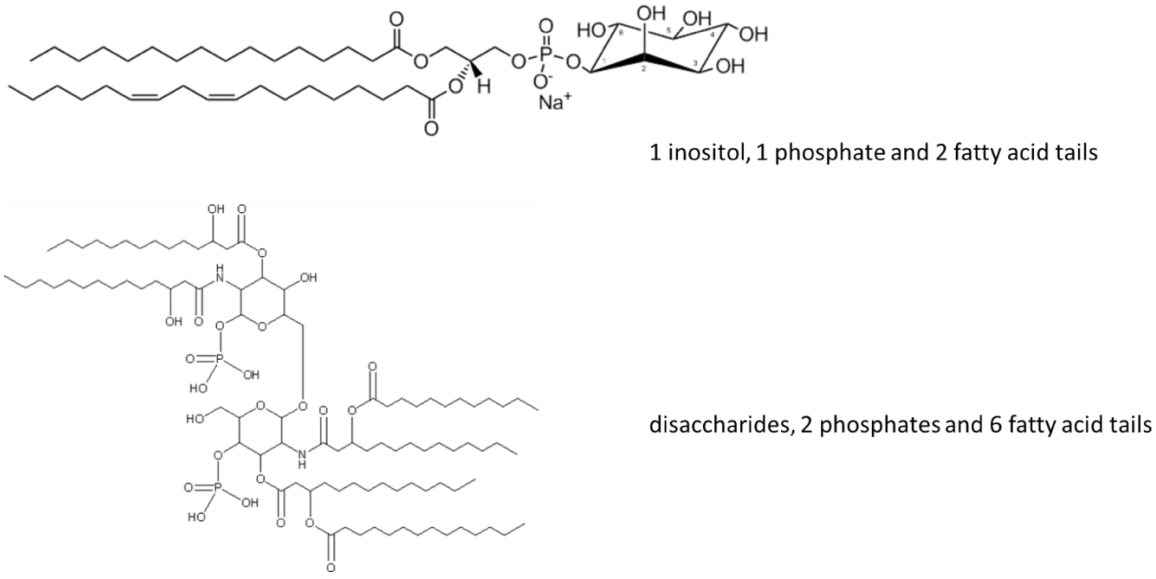

Figure 4-1. Structural comparison of phosphatidylinositol and lipid A.

Experiment

PI Incubation

PI powders were measured in vials and dissolved in 40% ACN at the concentration of 0.5mM directly, then vortexed until dissolved completely. TEM images of PI solution were taken every day. After PI assemblies into stable structure, PI solution and Aβ(16-22) solution were mixed and incubated.

Results

After incubation for several days, PI assembled into vesicles in 40% ACN, as shown in **Figure 4-2**.

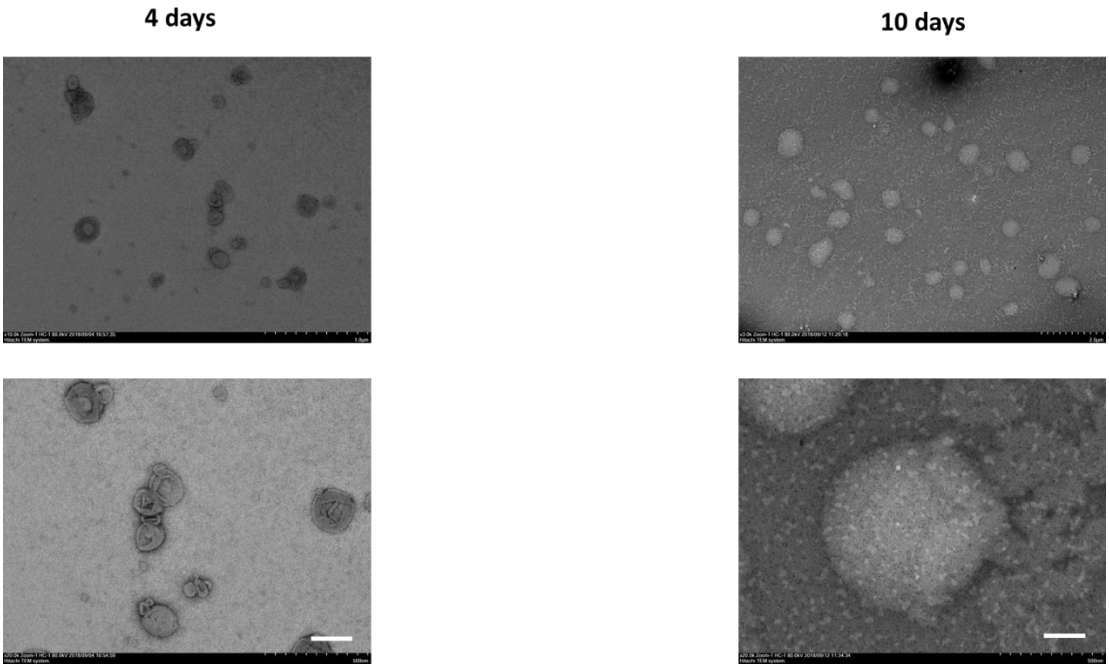

Figure 4-2. TEM images of 0.5mM PI in 40% ACN after 4days and 10days. Scale bar = 200nm.

Aβ(16-22) and PI assembly process

To explore the interaction between Aβ(16-22) and PI, two set of experiments were designed to examine their interaction at alkyl chain ratio equals to 1:1 and charge ratio equals to 1:1, respectively. Phenomena and TEM images were recorded every other day.

After mixing 0.5mM Aβ(16-22) with 0.25mM PI for about 5min, precipitates appeared in the vials, while mixture of 0.2mM Aβ(16-22) with 0.2mM PI maintained transparent for a long time. TEM images showed that in both conditions fibers bundled and twisted into large rods, though 0.5mM Aβ(16-22) with 0.25mM PI bundled quicker and forming rods with bigger diameters compared with 0.2mM Aβ(16-22) with 0.2mM PI. However, it is difficult to tell if peptide bundled with lipid together or peptide self-assembled under the influence of lipid to form such different structures from peptide self-assembly alone. **Figure 4-4** compared the structures among Aβ(16-22) self-assembly, lipid A-Aβ(16-22) assembly and PI-Aβ(16-22) assembly after 4 days. It is obvious that peptide fibers always bundled intensively in the presence of phospholipids, no matter lipid A or phosphatidylinositol, but their structures differed from one another.

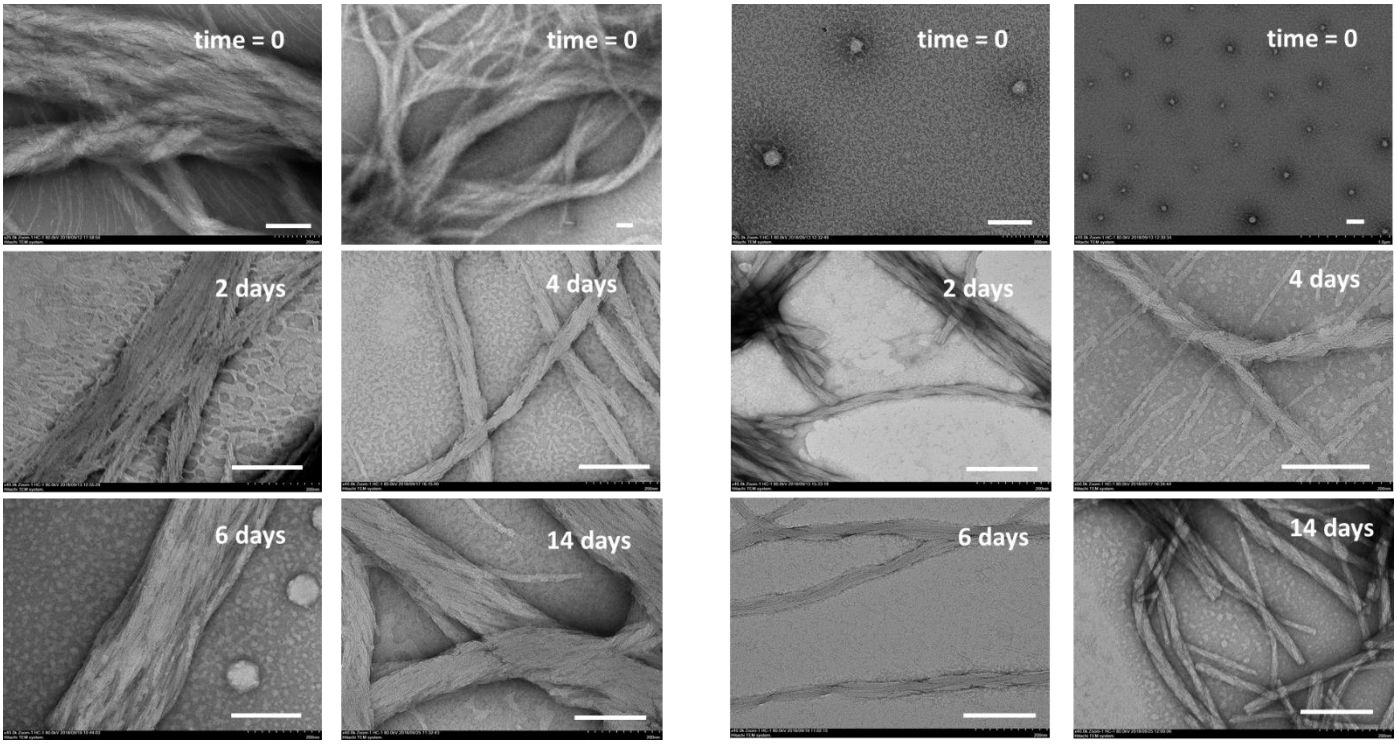

Figure 4-3. TEM showed the assembly process of PI and Aβ(16-22) at different concentration ratios. (a) chain ratio = 1:1, 0.5mM Aβ(16-22) with 0.25mM PI (left); (b) charge ratio = 1:1, 0.2mM Aβ(16-22) with 0.2mM PI (right). Scale bar = 200nm.

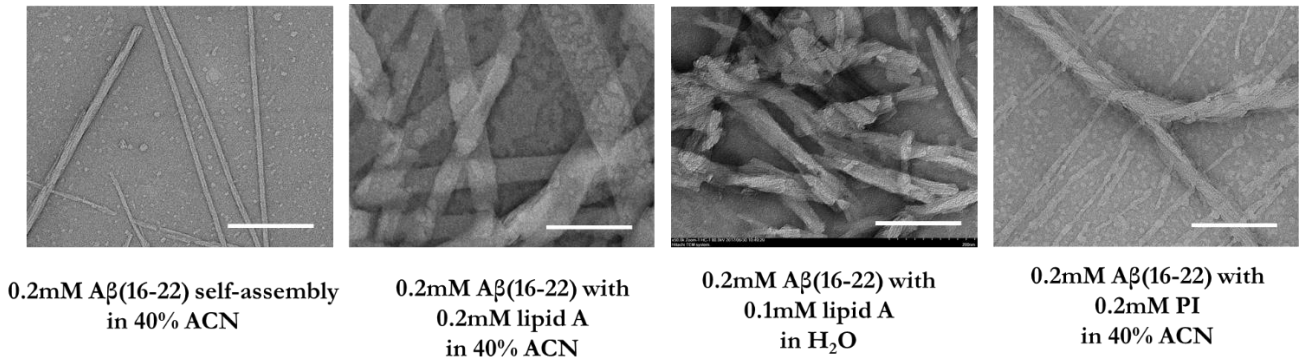

Figure 4-4. Comparison of Aβ(16-22) self-assembly, lipid A-Aβ(16-22) assembly and PI-Aβ(16-22) assembly structures after 4 days.

Conclusion

The results showed that phosphatidylinositol had the ability to induce the bundling and twisting of peptide fibers, which was consistence with the assembly between lipid A and amyloid.

Reference

(1) Choy, Christopher H., Bong-Kwan Han, and Roberto J. Botelho. "Phosphoinositide diversity, distribution, and effector function: Stepping out of the box." Bioessays 39.12 (2017): 1700121.

Chapter 5. Conclusion and perspectives

Introduction

There are some advanced techniques to characterize the structure of lipid/peptide assemblies and identify the interaction between lipid and peptide.

(a) Electrostatic Force Microscopy (EFM): In the EFM amplitude micrographs, positively charged surfaces are white and negatively charged surfaces are dark, thus mapping the charge distribution on the surface of lipid/peptide co-assembly and revealing the distribution pattern of lipid and peptide.

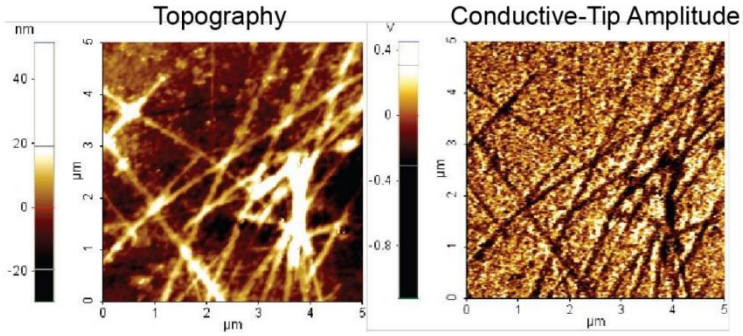

Figure 5-1. Atomic and electrostatic force microscopy images of (K16pY) (E22L) nanotube assemblies with surfaces coated by the positively charged protein. (**Left**) topography images of peptide nanotubes and (**Right**) EFM amplitude micrographs with a DC bias = +1V [2].

(b) Isotope-edited FTIR Spectra: The distribution between ^{12}C and ^{13}C bands in FTIR spectra reflects the extent of the packing along the entire β-sheets, which are diagnostic of the β-strand orientation and registry differences between lipid/peptide co-assembly and peptide self-assembly.

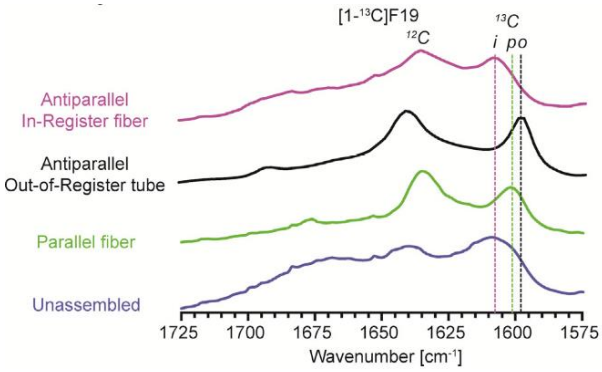

Figure 5-2. IE-IR spectra of mature, homogenous [1-^{13}C] F19 enriched peptides in antiparallel in-register (magenta), antiparallel out-of-register (black), and parallel [^{13}C] (green) strand orientations and unassembled (blue) peptide [3].

(c) Solid state NMR: Peptide registry in amyloid assemblies have been assigned definitively by ssNMR analyses and shown to correlate with isotope edited (IE) FT-IR analyses.

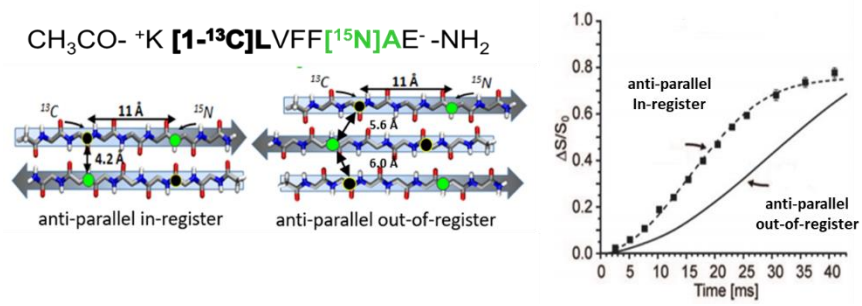

Figure 5-3. $^{13}C\{^{15}N\}$ REDOR and ^{13}C DQF-DRAWS solid-state NMR correlate with IR and showing the β-sheet register information [3].

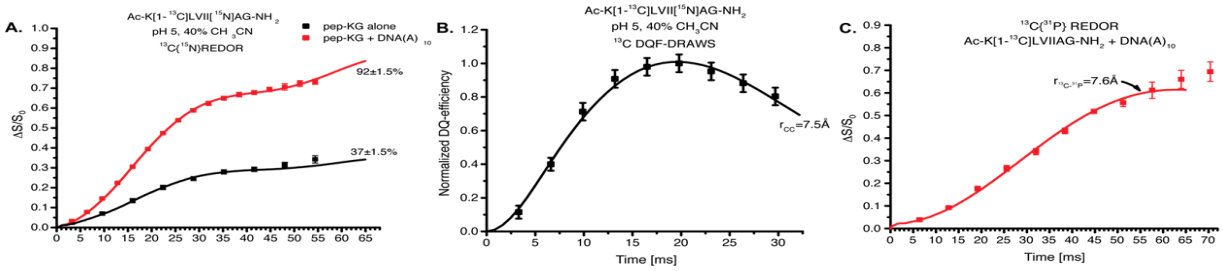

Figure 5-4. Structural characterization of DNA/Peptide co-assemblies. (A) $^{13}C\{^{15}N\}$ REDOR (B)^{13}C DQF-DRAWS (C) $^{13}C\{^{31}P\}$ REDOR [5].

(d) Confocal Fluorescence: ThT is a defining probe for β-sheet peptide assemblies as it displays increased fluorescence and a characteristic red shift of its emission spectrum upon binding to those assemblies [5]. With ThT fluorescence, the β-sheet structures in lipid/peptide assemblies are observed. With confocal fluorescence, merging of LPS and Aβ peptides are showed, thus proving the colocalization.

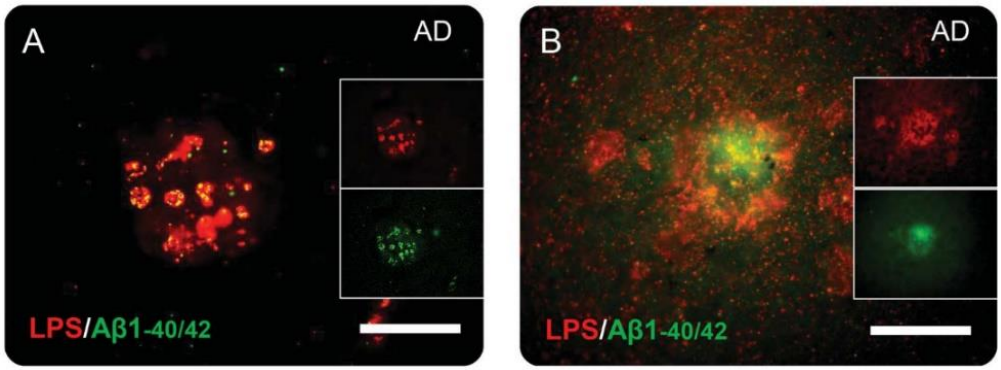

Figure 5-5. Association of lipopolysaccharide (LPS) with amyloid plaques in Alzheimer disease (AD) brains [6].

Conclusion

To demonstrate that bacterial membranes could induce the aggregation of amyloid peptide, which may be a cause of Alzheimer's disease, interaction between lipids and amyloid peptides were explored. In my experiments, I constructed the assemblies of lipid A/Aβ (16-22) and PI/Aβ (16-22) in both aqueous and organic solutions. Their structures were characterized with TEM and ATR-FTIR, showing the potential of lipid A-Aβ (16-22) co-assembly as a model to study the interaction between LPS and Aβ (1-40/42). My experiments also demonstrated the association between LPS and Aβ (16-22) by CD spectra, supporting LPS inducing of the β-sheet formation from unordered amyloid peptide. These data provide a possibility to explain the etiology of Alzheimer's disease with the bacterial effect.

Perspectives

Define the structure of lipid A/Aβ (16-22) assemblies

From the results of FTIR and CD, it is hard to define β-sheet registry of lipid A/Aβ (16-22) assemblies, which could be obtained from isotope-edited FTIR and $^{13}C\{^{15}N\}$ REDOR and ^{13}C DQF-DRAWS solid-state NMR (see **Figure 5-3**). Considering the chemical structure and properties of lipid A and Aβ (16-22), there are two possible models of lipid A/Aβ (16-22) co-assembly shown in **Figure 3-1**. Model a hypothesizes that lipid A can insert into the laminations of peptide β-sheets, so the d spacing of β-sheet lamination will be wider than the d spacing without lipid A insertion. This can be examined by X-ray diffraction. **Figure 5-6** gives an example of how diffraction of N-acyl-Aβ (16-22) peptide assemblies enlarges from 9.8 A to 11.5 A after the C_{12} alkyl chain inserts into the lamination of N-acetyl-Aβ (16-22). In contrast, if lipid A binds to the edges of peptide layers, as shown in model b, then the d spacing of β-

sheet lamination will not change. Also, multilayers are expected to form in model b, which can be characterized by TEM images, EFM mapping and confocal fluorescence to show the merging of lipid A and Aβ (16-22) layers. To further analyze the interaction between peptide backbones and lipid A headgroups, the distance between ^{13}C enrichment of the carbonyl of leucine or the N-terminal acetate and lipid A phosphate headgroups can be assigned in $^{13}C\{^{31}P\}$ REDOR (see **Figure 5-4**).

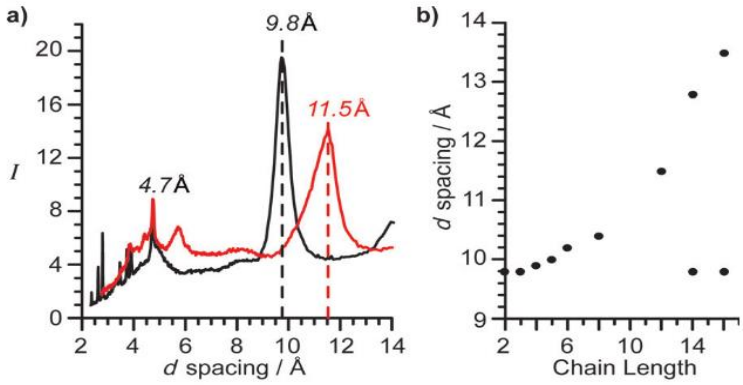

Figure 5-6. Powder and oriented electron diffraction of N-acyl-Aβ (16-22) peptide assemblies. a) X-ray powder diffraction of N-lauroyl-Aβ (16-22) (red) and and N-acetyl-Aβ (16-22) tubes (black) [1].

Extend the lipid A-Aβ (16-22) interaction to the LPS-Aβ (1-40/42) and bacterial membrane-Aβ (1-40/42) interaction

With the structure and interacting mechanism of lipid A-Aβ (16-22) co-assembly, I will extend this model to the interactions between LPS and Aβ (1-40/42) or even bacterial membrane and Aβ (1-40/42). However, the structure of LPS and bacterial membrane is much more complicated than lipid A, so perhaps similar results of diffraction and ssNMR will not be clear. In that case, I will consider using fluorescence to visualize the direct binding or inserting of Aβ peptides to LPS membrane. I will also

evaluate any correlation between the morphology of Aβ peptides, monomer, fibril or plaque, induced by the disruption of the bacterial membrane.

Reference

1. Ni, R., et al., *Remodeling Cross-beta Nanotube Surfaces with Peptide/Lipid Chimeras.* Angewandte Chemie-International Edition, 2012. **51**(27): p. 6635-6638.

2. Lu, K., et al., *Exploiting amyloid fibril lamination for nanotube self-assembly.* Journal of the American Chemical Society, 2003. **125**(21): p. 6391-6393.

3. Gawrisch, K. and B.W. Koenig, *Lipid-peptide interaction investigated by NMR.* Peptide-Lipid Interactions, 2002. **52**: p. 163-190.

4. Allisandra K. Rha, Dibyendu Das, Anil K. Mehta, Olga Taran, Yongang Ke, David G. Lynn, 2017. Structural insights on ribonucleoprotein (RNP) granule maturation and disease etiology (in progress)

5. Terzi, E., G. Holzemann, and J. Seelig, *Interaction of Alzheimer beta-amyloid peptide(1-40) with lipid membranes.* Biochemistry, 1997. **36**(48): p. 14845-14852.

6. Zhan, X.H., et al., *Gram-negative bacterial molecules associate with Alzheimer disease pathology.* Neurology, 2016. **87**(22): p. 2324-2332.